Review Article

Electrochemically driven dynamic plasmonics

Yan Jin,[a] Lin Zhou,[a,b,*] Jie Liang,[a] and Jia Zhu[a,*]
[a]Nanjing University, College of Engineering and Applied Sciences, National Laboratory of Solid State Microstructures, Jiangsu Key Laboratory of Artificial Functional Materials, Nanjing, China
[b]Nanjing University, Key Laboratory of Intelligent Optical Sensing and Manipulation, Ministry of Education, Nanjing, China

Abstract. Dynamic plasmonics with the real-time active control capability of plasmonic resonances attracts much interest in the communities of physics, chemistry, and material science. Among versatile reconfigurable strategies for dynamic plasmonics, electrochemically driven strategies have garnered most of the attention. We summarize three primary strategies to enable electrochemically dynamic plasmonics, including structural transformation, carrier-density modulation, and electrochemically active surrounding-media manipulation. The reconfigurable microstructures, optical properties, and underlying physical mechanisms are discussed in detail. We also summarize the most promising applications of dynamic plasmonics, including smart windows, structural color displays, and chemical sensors. We suggest more research efforts toward the widespread applications of dynamic plasmonics.

1 Introduction

Plasmonics, with the unique capability of flexible steering on electromagnetic waves down to the nanoscale,[1–4] is beneficial for potential applications, such as bio-sensors, integrated optical information devices,[5–10] and solar energy conversion.[11–15] In the past decades, various nanostructures have been successfully demonstrated to precisely control the optical field or spectroscopy.[16–20] However, most conventional plasmonic designs are passive devices with static microstructures and fixed optical properties, which can hardly meet all of the real-time demands. Dynamic plasmonics, sometimes called reconfigurable plasmonics or programmable plasmonics, is regarded as one of the most promising branches of plasmonics apart from the passive ones, in which plasmonic structures and their optical responses can be actively tuned by external fields. In the past decades, dynamic plasmonics has garnered considerable interest in the disciplinary fields of physics, chemistry, and material science. Dynamic plasmonics has in turn triggered versatile fabrication approaches and held great promise for applications in smart devices and chemical detection.

Thus far, there are several classic reviews that are devoted to the field of dynamic plasmonics.[21,22] Several strategies have been proposed for dynamic plasmonics, including electrical controls by carrier doping (graphene)[23–25] or refractive index manipulation [liquid crystal (LC)][26] with the applied voltage, chemical reactions by varying the pH value and biological species,[27–30] electrochemical redox reactions by manipulating structures or carrier-densities of plasmonic materials themselves or surrounding materials,[31–37] thermal stimuli by phase-change materials (such as vanadium dioxide) and thermo responsive polymer materials [such as poly(methyl methacrylate)],[38–43] mechanical strains by varying microstructures (such as period or distance between periodic plasmonic structures) through the flexible polymers substrate (such as polydimethylsiloxane),[44–47] optical excitations with photochromic molecules and quantum dots,[48–51] and magnetically driven approaches with magneto-plasmonic systems combining noble metals and ferromagnetic components (for example, Au–Fe$_3$O$_4$ nanostructures).[52–55]

Among the above-mentioned versatile dynamic-control strategies, electrochemically driven dynamic plasmonics, which serves as an intermediate approach between pure electric controls and chemical reactions, not only features flexible on-chip integration but also benefits from versatile chemical transformations, inspiring more extensive research interest and a broad

*Address all correspondence to Lin Zhou, linzhou@nju.edu.cn; Jia Zhu, jiazhu@nju.edu.cn

range of potential applications. With the extensive development of nanoscience/nanotechnology in electrochemistry, electrochemical methods provide an effective pathway to enable dynamic plasmonics almost covering the entire optical window, ranging from the visible to near-infrared (NIR) wavelength. The redox reactions with inherent introduction of energy storage possess the self-powered capability of the dynamic plasmonics for potential applications in smart devices.

Despite intriguing advancements in the past decade, the field of electrochemically driven dynamic plasmonics has been encountering a number of challenges as well. At the intersection of electric and chemical strategies, electrochemical dynamic plasmonics has the common disadvantages of both strategies as below. On the one hand, the electric control (especially, the electric field distributions) inside an electrochemical system is inevitably affected by the electrolytes and chemical reactions. On the other hand, the chemical reactions may be controlled by the electrodes under the applied electric field. All of the interactions will probably affect the efficiency, complexity, and durability of electrochemical dynamic plasmonic systems. Hence, the advantages and gaps in the knowledge of electrochemically driven dynamic plasmonics highlight the importance and urgency for a timely review summary of this important and relatively new direction of photonics.

Therefore, in this review, we focus on the recent advancements and future work on electrochemistry driven dynamic plasmonics. We summarize and discuss the main solutions to enable dynamic control of plasmonics [Figs. 1(a)–1(c)], including structural transformation, carrier-density modulation, and electrochemically active surrounding-media manipulation. These three approaches can dynamically control the resonant wavelength and intensity of optical spectra, which can potentially develop new optical applications. Subsequently, we review three main applications of dynamic plasmonics [Figs. 1(d)–1(f)]: smart windows, structural color displays, and chemical sensors. In addition, we also discuss the outlook and future work for the field of dynamic plasmonics.

2 Approaches to Realize Dynamic Plasmonics

The optical responses of a dynamic plasmonic system can be actively tuned via external fields. In the past few years, a large number of advancements that fully utilize versatile external fields have been developed to dynamically manipulate the plasmonic materials and/or microstructures, which finally results in the dynamic manipulation of the optical responses. Before going into detailed dynamic tuning approaches, we first discuss the fundamental basis of the tuning mechanisms for dynamic plasmonics, which are primarily based on solid materials such as metals and highly doped semiconductors. For materials with high density of free carriers, the interplay between long range Coulombic interaction and inertia of free carriers results in the unique elementary excitation quanta called (bulk) plasmon, the frequency of which is determined by the conductive carrier density n,

$$\omega_p = \left(\frac{ne^2}{m\varepsilon_0}\right)^{1/2}. \tag{1}$$

When it comes to the collective oscillation of free carriers near the material interfaces, it turns out to be the surface plasmon with the resonant frequency expressed as

$$\omega_{sp} = \omega_p/(1 + \varepsilon_s)^{1/2}. \tag{2}$$

Basically, as the incident light is shed on the plasmonic material, a nanometer scale penetration depth makes it only couple with the surface elementary excitation, generating surface
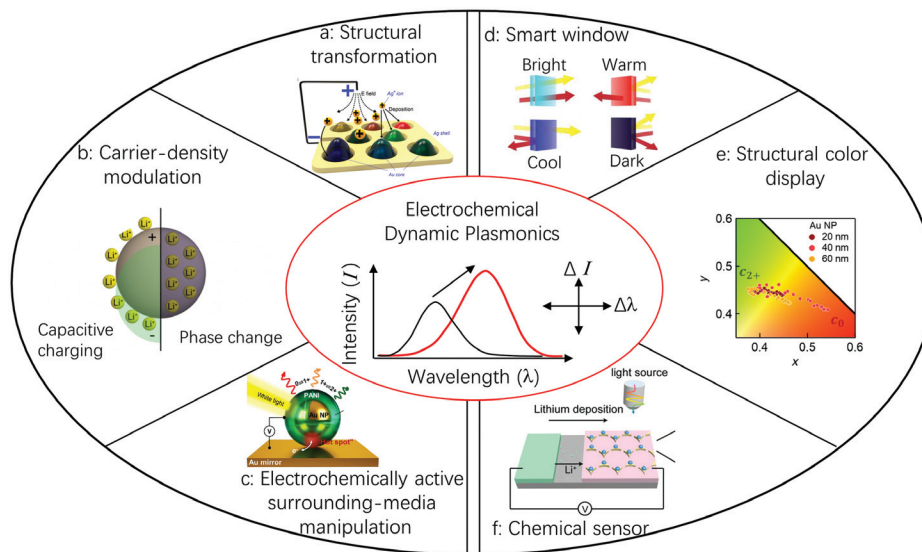

Fig. 1 Overview of electrochemistry enabled dynamic plasmonics: (a)–(c) approaches to realize dynamic plasmonics and (d)–(f) applications of dynamic plasmonics. (a) Reproduced with permission from Ref. 32, Copyright 2016, American Chemical Society. (b), (d) Reproduced with permission from Ref. 56, Copyright 2015, American Chemical Society. (c), (e) Reproduced with permission from Ref. 57, Copyright 2019, American Association for the Advancement of Science. (f) Reproduced with permission from Ref. 58, Copyright 2018, National Academy of Sciences.

plasmon polaritons (SPPs) along the continuous dielectric/plasmonic material interface once momentum conservation is satisfied. The wavevector and wavelength of SPPs can be written as[1]

$$k_{\text{spp}} = k_0[\varepsilon_m\varepsilon_s/(\varepsilon_m + \varepsilon_s)]^{1/2}, \tag{3}$$

$$\lambda_{\text{spp}} = \lambda_0/[\varepsilon_m\varepsilon_s/(\varepsilon_m + \varepsilon_s)]^{1/2}, \tag{4}$$

while the coupling that happens between the light and finite-sized curved plasmonic nanoparticles can lead to the generation of localized surface plasmon (LSP) resonances. Taking a spherical nanoparticle, for example, the wavelength of the LSP can be determined by the Mie scattering cross section,[1]

$$\sigma_{\text{sca}} = \frac{8\pi}{3}k_0^4 a^6 \frac{(\varepsilon_m' - \varepsilon_s)^2 + \varepsilon_m''^2}{(\varepsilon_m' + 2\varepsilon_s)^2 + \varepsilon_m''^2} \tag{5}$$

or

$$\lambda_{\text{LSP}} = \lambda_p(2\varepsilon_s + 1)^{1/2}, \tag{6}$$

where λ_p is the plasma wavelength of the plasmonic material; k_0 and λ_0 are the wavevector and wavelength of light in free space; $\varepsilon_m = \varepsilon_{m'} + i\varepsilon_m''$ and ε_s are the dielectric functions of the plasmonic material and the surrounding media, respectively; a is the diameter of the nanoparticle.

It is of no surprise that the spectral response of both SPP and LSP is highly dependent on the geometry shape and size of plasmonic microstructures, the free carrier density of the plasmonic materials, and the dielectric function of the surrounding media, which form the primary tuning parameters and potential mechanisms for dynamic plasmonic systems. Therefore, we discuss three primary tuning approaches for dynamic plasmonics through electrochemical reactions: structural transformation, carrier-density modulation, and electrochemically active surrounding-media manipulation. We review the detailed theoretical designs and optical properties of each method in the following section one by one. It is worth noting that there are a couple of degrees of freedom for manipulating an arbitrary plasmonic system, such as amplitude, phase, wavelength, polarization, etc. In this review, we mainly focus on the amplitude- and wavelength-dependent spectroscopic manipulation for the sake of the structure complexity and effectiveness of electrochemical processes.

2.1 Structural Transformation

Plasmonic structures can be actively transformed by electrochemical metal deposition/stripping and particle assembly/disassembly electrochemical processes. More specifically, the shape, size, and interdistance of metal particles or the thickness of metal films can be flexibly tuned during the electrochemical processes. Here, we summarize the main progress of electrochemical metal deposition/stripping and particle assembly/disassembly processes for dynamic plasmonics, respectively.

Metal deposition/stripping is the first typical representative for the structural transformation. The metal can be electrically deposited and then removed through electrochemical reduction and oxidation reactions, respectively, leading to reconfigurable structures and thus reversible optical responses. The electrochemical metal deposition and stripping can thus flexibly engineer the spatially resolved spectroscopy. Here, we summarize electrochemical deposition/stripping enabled spectral modulation on the optical intensity and wavelength of plasmonic resonances as well as optical phase transitions that are primarily originating from the structural transformation.

Manipulation of spectral intensity of plasmonic responses by structural transformation of metallic structures is the most straightforward case and extensively demonstrated by electrochemical processes. Disordered metal deposition in aqueous electrolyte systems has attracted tremendous attention because of its safety, environmental friendliness, and transparency. Barile et al.[34] report the Cu-Pb or Cu-Ag deposition systems to successfully demonstrate the reversible transparency change. The high extinction coefficients of metals make it possible for the structure to enable highly opaque states with the ultrathin thickness of only tens of nanometers, beneficial for ultracompact dynamic devices. Taking the Cu-Pb system for example, Cu and Pb metal deposition happens at -0.55 V versus Ag/AgCl, with transmission efficiency reducing to 18% after 15 s because of light absorption with non-smooth metal films. Metal dissolution happens at $+0.65$ V to oxidize Cu and Pb to Cu^{2+} and Pb^{2+}, during which process the initial transmittance value can be recovered by 92% within an extra 15 s.

Apart from wavelength-independent spectral intensity manipulation in disordered plasmonic systems, structural transformation via electrochemical processes has also successfully been employed for wavelength-dependent spectral manipulation in well-defined electrodeposited metallic structures. Wang et al.[32] investigated the electrodeposition of periodic bimetallic Au/Ag nanodot arrays, which leads to ultrasensitive spectral response in the form of a fast plasmonic resonance shift as a function of structure parameters in the full-visible range. Through an electrodeposition process, Ag shells can deposit and dissolve on Au nanodomes to reversibly form Au/Ag core–shell structures, as the schematic shown in Fig. 2(a). The Au/Ag core–shell structures are designed because both the geometric factor and material (Ag shell) can lead to the blueshift for a wide tuning range. By varying the Ag thickness from 0 to 30 nm with different deposition times, simulation results of two-dimensional reflection spectra indicate that the resonant wavelength of the LSP can be continuously shifted from 670 to 450 nm [Fig. 2(b)]. Measured reflection spectra of the structures also show the remarkable blueshift (peak wavelength tuned from 650 to 430 nm), which agrees well with the simulation results [Fig. 2(c)].[32]

It is worth noting that most of the structural transformation-based electrochemical dynamic plasmonic systems are limited to noble metal structures thus far. There are commonly three considerations for noble metals systems: (1) most stable, (2) most well-known plasmonic materials with clear optical properties, and (3) mature fabrication processes. However, there are intrinsic drawbacks existing in noble metal-based electrochemically driven dynamic plasmonic systems, such as high cost, inherent optical loss, heavy and/or large ion sizes, etc., making their commercial applications illusive. Recently, alkali metals have drawn considerable interests in the field of dynamic plasmonics because of their unique priorities: (1) excellent optical properties are comparable to or even better than noble metals (especially, lower optical loss).[60,61] (2) Lighter alkaline metals may show faster mobility and thus faster optical response. (3) New fabrication processes are possible due to unique properties of alkaline metals. For example, the relatively low melting point of sodium metal
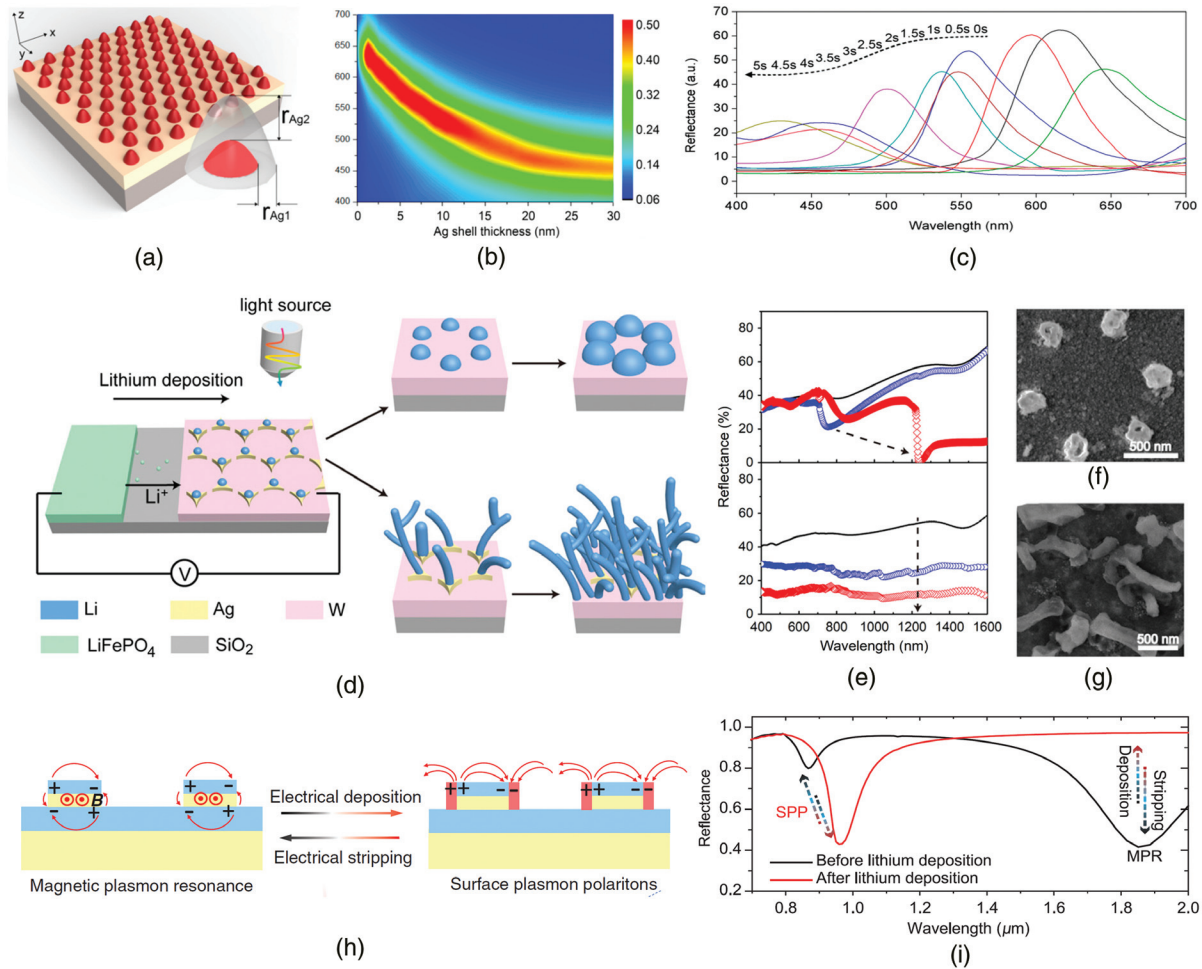
Fig. 2 Structural transformation for dynamic plasmonics. (a) Schematic of Au/Ag nanodome arrays. (b) Simulation of two-dimensional reflection spectra as a function of Ag shell thickness. (c) Measured reflection spectra of the device after different electrodeposition times. (d) Schematic of the morphology evolution during lithium deposition at different applied currents: lithium particle growth and disorder lithium dendrite formation. (e) Simulation reflectance of two lithium morphologies: shifts of reflectance dip and suppressed reflectance intensity. (f) The scanning electron microscope (SEM) image of lithium particles. (g) The SEM image of lithium dendrites. (h) Schematic of selective lithium deposition transferring metal–insulator–metal to the semi-infinite metallic grating. (i) The corresponding calculated reflection spectra switching between MPR and SPP. (a)–(c) Reproduced with permission from Ref. 32, Copyright 2016, American Chemical Society. (d)–(g) Reproduced with permission from Ref. 58, Copyright 2018, National Academy of Sciences. (h), (i) Reproduced with permission from Ref. 59, Copyright 2020, Wiley-VCH GmbH.

induces the hot spin-coating fabrication process for sodium plasmonic structures.[62] (4) Alkali metals are the most important materials for energy storage systems (alkaline metal batteries).[63–66] Li metal is regarded as the holy grail of anode materials for high-energy-density lithium metal batteries because of its highest energy density (3860 mAh g^{-1}) and lowest electrochemical potential (-3.04 V versus the standard hydrogen electrode). Thus, benefiting from the combination of two unique features of alkali metal (important information and energy storage carriers), alkali metal-based dynamic plasmonics is an important step toward energy-saving/self-powered smart devices.

Very recently, wavelength- and intensity-resolved plasmonic spectral manipulation has been successfully demonstrated in lithium metal batteries with different applied currents by Jin et al.[58] [Fig. 2(d)]. Wavelength-dependent dynamic plasmonics is achieved by structural transformation through selective ordered lithium particle nucleation and growth in the reasonable current range. With the growth of lithium particles (diameter of lithium particles increases from 200 to 350 nm, with the increase of deposition time), size-dependent pronounced asymmetric reflective dips shift from ~800 to 1200 nm [Figs. 2(e) and 2(f)]. This can be ascribed to the hybridizations of the LSP (related to the isolated lithium particles) and Wood's anomaly (WA, related to the periodic geometry), with amplified LSP observed around $WA_{1,0}$ at ~1230 nm and $WA_{1,1}$ at ~710 nm. Furthermore, the reflectance dip shift is reversible during the lithium stripping

process in the full cycle of lithium metal batteries. Wavelength-independent intensity manipulation was realized at a large current with the undesirable disordered lithium dendrites formation [Figs. 2(e) and 2(g)]. Plasmonic light trapping by light scattering and coupling properties of lithium dendrites exhibits a flat spectroscopic profile with only reflection intensity suppression.

Furthermore, Jin et al.[59] combined alkali metals and noble metals to enable the electrochemically driven optical "phase" transition. Dynamic plasmonic switching between magnetic plasmon resonance (MPR) and SPP excitations is achieved through structural transformation by selective lithium deposition on a metal–dielectric–metal (MIM) structure [Fig. 2(h)].[59] Through lithium deposition in a lithium metal battery, the periodic Ag-SiO_2-Ag MIM grating structure transfers to a continuous donut geometry, leading to the optical switch from localized MPR excitations (MPR, 1.8 μm) to delocalized electric excitations (SPP, 0.8 μm) in Fig. 2(i). This switch is reversible by the lithium stripping process in a full electrochemical cycle.

The second typical representative for structural transformation-based dynamic plasmonics is the nanoparticle assembly/disassembly at the interphase of two immiscible electrolyte solutions inside an electrochemical cell. Specifically, with the negative voltage applied to the aqueous solution relative to the organic solution, the nanoparticle will assemble at the interphase and increase particle density, leading to redshifted high reflectivity. Upon reversing the potential to positive for aqueous solution, the nanoparticle will disperse in aqueous solution and lead to blueshifted reflectance and finally increase transmittance. The voltage control can guide the reversibility between a highly reflective "mirror" to a transmissive "window."[67] Furthermore, the nanoparticle assembly/disassembly enabled dynamic plasmonics can be extended to new designs/structures, including metal nanocuboids,[68] Fabry–Perot interferometers, 3D superstructures,[69,70] and different substrates (the interphase of liquid and dielectric/metal film substrates).[71,72] For theoretical understanding, refer to Refs. 73 and 74, in which several factors were taken into consideration, including nanoparticle dimensions, interparticle separation, metal film thickness, the gap between the film and nanoparticles, and incident light characteristics. For more details and recent progress of the nanoparticle assembly/disassembly enabled dynamic plasmonics, refer to specific review papers, such as Refs. 75–78.

2.2 Carrier-Density Modulation

Aiming at directly tuning the plasma frequency of plasmonic materials, carrier-density modulation is the second effective way toward dynamic manipulation of plasmonic responses. In the experiment of an arbitrary electrochemical process, carrier-density modulation can be achieved by the capacitive charging process through the electrochemical injection or extraction of electrons into or out of plasmonic materials. In this section, we summarize two representative types of bulk plasmonic materials that can work in the optical regime: metal and transition metal oxide nanocrystal materials.[36,56,79] The difference between these two materials is the intrinsic free carrier density, which is up to 10^{23} and 10^{21} cm^{-3} for metal and highly doped transition metal oxide nanocrystals, respectively.[79]

The Drude model can be employed to quantify the shift of plasmonic resonance with the change of carrier density via electrochemical potential control, with the LSPR frequency decreasing as the carrier density decreases.[1] Ag colloids first

realized the LSPR shift through electron injection and extraction in 1991 by Henglein et al.[80] With −0.4 V versus Ag/AgCl negative potential applied to colloidal Ag [Fig. 3(a)], 1600 ± 300 electrons are transferred simultaneously to the metal particle. This leads to the resonance wavelength shift from 400 nm at a redox potential of +0.15 V versus Ag/AgCl to about 392 nm at −0.6 V versus Ag/AgCl [Fig. 3(b)].[81] The wavelength of the plasmon peak and the number of electrons transferred of the colloidal silver surface as a function of potential are demonstrated in Fig. 3(c). In addition, the modulation of the carrier density depends on the morphology of nanostructures. For example, metal nanostructures with smaller volume show larger modulation ability for carrier density change, and spectral shifts are more sensitive for anisotropic nanoparticles, such as nanorods.[83] The 11-nm blueshift in scattering spectra of a single gold nanorod can be reversibly achieved.[84] Moreover, there are other effects that happen along with the changes of carrier density, such as the changes of surface damping and the modified dielectric function of particle shells.[85] However, because of the high intrinsic carrier concentration of Ag colloids (10^{23} cm^{-3}), the wavelength shift of metal-based plasmonics is rather limited.

Compared with metal nanocrystals, larger optical modulations can be achieved in transition metal oxide nanocrystal materials. Transparent conducting oxides, including tin-doped indium oxide (ITO) and aluminum-doped zinc oxide (AZO) [Figs. 3(d) and 3(e)], exhibit suitable carrier concentrations (∼10^{21} cm^{-3}) with plasma frequencies in the NIR region. Thus, the optical shift of doped transition metal oxide nanocrystals can be higher than metals. In addition, the optical modulation in the NIR region can control the solar energy transmittance and can be used in applications for smart windows (discussed in detail in Sec. 3.1). With the applied voltage changing from 2 to 4 V for ITO, the solar transmittance increases from 78% to 91%, and NIR solar transmittance increases from 56% to 81% [Fig. 3(g)]. The optical contrast is higher in the case of AZO. With the voltage changing from 1.5 to 4 V for AZO, the solar transmittance increases from 62% to 82%, and NIR solar transmittance increases from 38% to 77% in 0.1 M (1 M = 1 mol/L) $LiClO_4$ in propylene carbonate electrolyte [Fig. 3(f)].[82]

Furthermore, dual-modulations or optical phase transitions were realized in a single material—niobium-doped anatase TiO_2 nanocrystals in the visible and NIR range separately, proposed by Dahlman.[56] TiO_2 is a commonly studied electrode material for lithium ion batteries. The energy storage mechanism is the reversible lithium ion insertion/extraction and related phase changes. In addition, niobium-doped anatase TiO_2 nanocrystals [Fig. 3(h)] possess LSPR in the NIR range. The optical property at three different voltages states is systematically studied [Fig. 3(i)]. At 3.5 V (versus Li/Li$^+$), TiO_2 is at the oxidation state with transparent visible and NIR spectra as the "bright" state. With the applied external voltage, the voltage of the TiO_2 electrode reduces to 1.8 V, approaching the constant voltage plateau. Electrochemical injection of electrons can dynamically change the carrier intensity and spectral position of LSPR absorption at the NIR range. The capacitive charge induces infrared extinction and leads to the "cool" state. At the fully reduced state with the voltage at 1.5 V, the lithium insertion leads to phase change from the anatase titanium oxide to the distorted orthorhombic $Li_{0.5}TiO_2$ phase. With lithium insertion, localization of injected electrons exists on Ti cations, creating a polaronic lattice distortion, which is similar to electrochromic
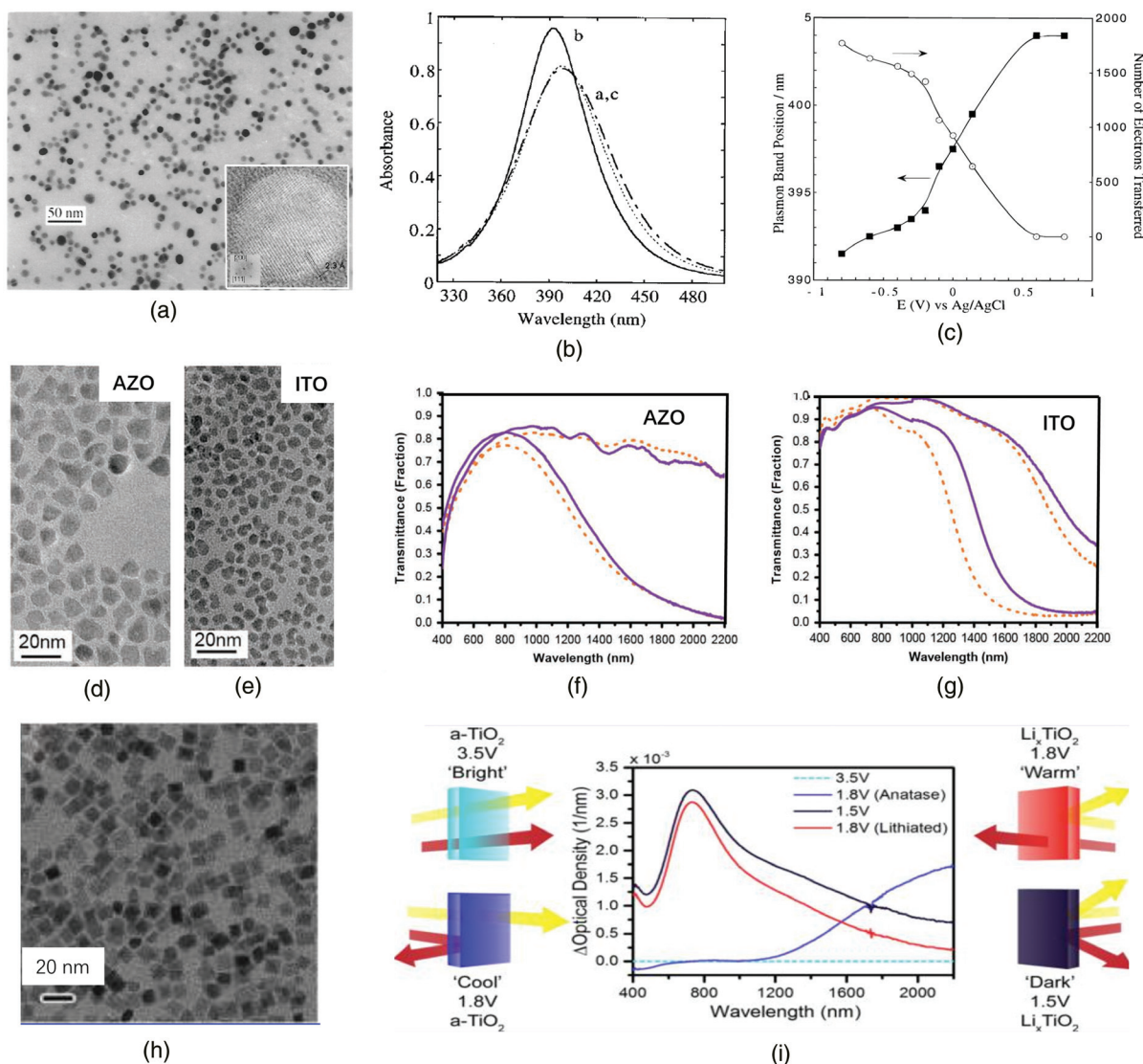
Fig. 3 Carrier-density modulation for dynamic plasmonics. (a) The SEM image of the colloidal silver particles. Inset is the transmission electron microscopy (TEM) image. (b) Absorption spectra of the silver solution at the open circuit potential of (a) +0.15 V, (b) –0.6 V, and (c) +0.15 V versus Ag/AgCl. (c) The position of the plasmon peak and number of electrons transferred of the colloidal silver surface as a function of potential. TEM images of (d) AZO and (e) ITO nanocrystals. The transmittance of (f) AZO and (g) ITO nanocrystals before (orange, dashed) and after 20,000 cycles (purple, solid) with voltage modulation. (h) The TEM image of 5% Nb-doped TiO$_2$ nanocrystals. (i) *In situ* spectroelectrochemistry of 5% Nb-doped TiO$_2$ films with four distinct optical states, with different transmittance of visible (yellow arrow) and infrared (red arrow) light. (a)–(c) Reproduced with permission from Ref. 81, Copyright 1997, American Chemical Society. (d)–(g) Reproduced with permission from Ref. 82, Copyright 2013, Wiley-VCH Verlag GmbH & Co. (h), (i) Reproduced with permission from Ref. 56, Copyright 2015, American Chemical Society.

mechanisms in conventional transition metal oxides, such as WO$_3$. Ti^{3+} polaronic color centers result in visible extinction as the "dark" state. Lastly, capacitive oxidation can dismiss the NIR extinction and forms the "warm" state.

2.3 Electrochemically Active Surrounding-Media Manipulation

In addition to manipulating the optical response of a plasmonic system directly by steering the nanostructures or intrinsic properties of the plasmonic material itself, a third pathway to achieve dynamic plasmonics is to actively control the optical property of the surrounding materials of the target plasmonic structures. The effective refractive index of the compound plasmonic structures can be flexibly tuned by external electric fields. One of the most representative cases is the electrochromic materials, including inorganic tungsten oxide (WO$_3$) and organic polymers.[26,33,86–89] Two effective strategies for dynamic control of the refractive index of electrochromic materials are ion insertion and redox reactions of polymers.

Ion injection into the surrounding media can be a powerful way to electrically tune the plasmonic resonances. H^+, Li^+, Na^+, and multivalent-ions (including Zn^{2+}, Mg^{2+}, and Al^{3+}) insertion into WO_3 (the most widely studied conventional inorganic electrochromic material) can tune the refractive index and extinction coefficient of WO_3 from 2.1 to 1.8 and 0 to 0.5, respectively. A combination of WO_3 and plasmonic nanostructures can tune the plasmonic resonance wavelength. Metal–insulator–nanohole cavities with WO_3 as the insulator layer show the resonance wavelength modulation from 601 to 505 nm (64-nm peak wavelength shift achieved in the experiment) during lithium insertion [Figs. 4(a)–4(d)].[37]

Optical phase change of surrounding media is the second route to dynamically tune its refractive index and thus plasmonic responses of the overall metallic structures. For example, the electrochromic polymer shows a reversible manipulation of the refractive index through electrochemical reduction or oxidation by applying a small voltage. Peng et al.[57] reported that the 0- to 20-nm polyaniline (PANI)-coated Au nanoparticle on a metallic Au mirror can demonstrate tunable scattering [Fig. 4(e)]. The inset SEM image shows an 80-nm Au nanoparticle coated with 20-nm PANI shell on an Au substrate. In the voltage range of −0.2 to 0.6 V versus Ag/AgCl, >100-nm resonance wavelength shift is demonstrated in Figs. 4(f) and 4(g) (the parameter for display application is summarized in Sec. 3.2).[57] However, realizing full color control by a single structure is still difficult. Xu et al.[86] reported plasmonic electrochromic switchable configurations based on arrays of metallic nanoslits and electrochromic polymer. The 25-nm PANI polymer film coated on the Au-nanoslit array shows the high optical modulation amplitude with 80% switch contrast and fast switching time of 9 ms. Applying different periods of metallic nanoslit arrays (from 390 to 240 nm) with PolyProDOT-Me_2 polymer, full color from red to blue at the on state is demonstrated. The off state is totally black, proving the tunability.[86]

2.4 Hybrid Manipulation

Inspired by the three main manipulation approaches discussed above, hybrid manipulation has been employed for dynamic plasmonics as well. For example, by combining the structural transformation with surrounding-media manipulation, recently, metal reduction/chlorination redox reactions have been proposed by Byers et al.[90] in Au/Ag core–shell systems for gradual optical spectral manipulation. Ag-AgCl conversion can not only transfer structures by reduction reactions but also change the refractive index of surrounding materials by chlorination reactions for dynamic plasmonics. For individual Au/Ag core–shell nanoparticles, the electrochemical reduction reaction (AgCl to Ag) results in the particle size increment and the refractive index of surrounding media changing from AgCl [$n_{AgCl(s)} = 2.02$] to the electrolyte ($n_{electrolyte} = 1.34$), leading to the increased scattering intensity and shifted plasmonic resonances. For coupled Au/Ag core–shell dimers, Ag-AgCl redox reactions can effectively change the gap width of the dimers and convert shell-dominated resonance (Ag shell) to core-dominated resonance (AgCl shell). By further increasing the Ag shell thickness through electrochemical reduction reactions, the direct contact
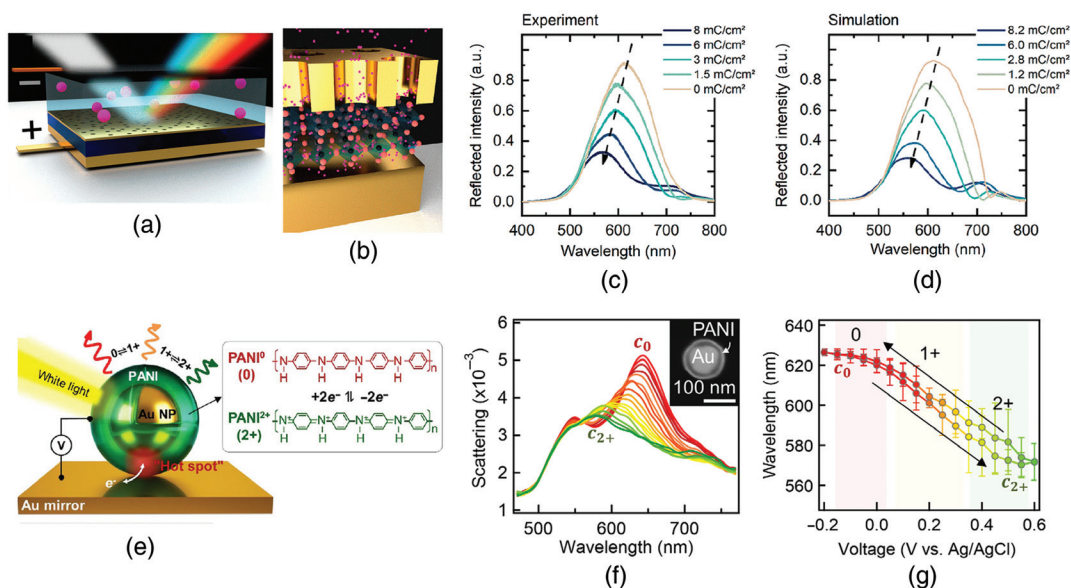

Fig. 4 Electrochemically active surrounding-media manipulation for dynamic plasmonics. (a)–(d) Schematic, experimentally obtained reflectance spectra and FDTD simulated reflectance spectra of plasmochromic nanocavities based on a WO_3 insulator layer with lithium insertion. (e) Schematic of a PANI-coated Au nanoparticle on a metallic Au mirror and redox reaction of PANI (PANI[0], fully reduced; PANI[1+], half oxidized; PANI[2+], fully oxidized). (f) Scattering spectra and inset SEM image of a single PANI-coated Au nanoparticle (c_0, PANI[0]; c_{2+}, PANI[2+]). (g) Reversible switching of coupled plasmon resonance wavelength versus the applied voltage. (a)–(d) Reproduced with permission from Ref. 37, Copyright 2020, American Chemical Society. (e)–(g) Reproduced with permission from Ref. 57, Copyright 2019, American Association for the Advancement of Science.

of the dimer happens, accompanied by electron-tunneling-induced charge transfer as well as plasmonic switches from capacitive to conductive coupling, leading to the optical phase change.[90]

The above-summarized approaches for dynamic plasmonics are reversible, which are highly desired for most potential applications that are discussed in Sec. 3. However, it is worth noting that the irreversible electrochemical reactions and related structural transformation are unavoidable in electrochemistry. This can also lead to dynamic plasmonics that may be useful for fundamental investigations and/or specialized applications. The typical representative is metal dissolution. With the applied positive electrochemical potential, metal is dissolved with an absorbed halide anion, which can change the structure (volume and aspect ratio) of nanostructures, tuning the intensity, peak wavelength, and full width at half-maximum of optical spectra. The behavior can be observed in nanoparticles, nanorods, nanodimers, and Au lattices.[91–94] The rate of electrodissolution can be adjusted (accelerated by laser excitations with hot holes,[95] inhibited with low concentrations of oxoanions[96]). Under potential deposition (UPD)[97] technologies can also be applied for metal dissolution of Au dimer structures.[93] In addition, the surface properties of metal structures during the UPD and stripping process are not reversible. Ag UPD and stripping on polycrystalline Au film lead to the rearranged Au film due to strong adatom–substrate interactions, with obvious change of n (0.133, 0.565), k (3.6, 9.39) of Au film before and after 27 times UPD and stripping.[98,99]

3 Potential Applications of Dynamic Plasmonics

By flexibly engineering the microstructures and constituting materials of plasmonic systems, dynamic plasmonics can enable the powerful manipulation of spectral or optical fields, which would be promising for a variety of applications in optoelectronic devices.[100] Due to the unique properties of electrochemical strategies for dynamic plasmonics, such as the electronic compatible controls, simultaneous manipulation of information components, and energy storage, the potential applications of electrochemical-based dynamic plasmonics may inspire some distinctive devices. We summarize three potential applicable directions of dynamic plasmonics: smart windows, structural color displays, and chemical sensors.

3.1 Smart Windows

The smart window is an emerging technology to adjust the transmittance of the ultraviolet (UV), visible, and infrared solar irradiance in buildings and sunroofs of vehicles, which can save an average of 10% energy compared to traditional static windows, mainly because of the reduced lighting, heating, and cooling costs. The primary requirement of smart windows is the reversible transparency change at the on and off states triggered by electro-, thermo-, or photo-stimulations.[101] One of the widely employed materials for commercial smart windows is inorganic electrochromic materials. Dynamic plasmonic systems feature the high optical contrast, high reversibility, and excellent durability of controllable transparency in the wavelength of visible and NIR ranges. Thus, reversible dynamic plasmonic devices are inherently ideal candidates for smart windows. Among the three above-discussed approaches for dynamic plasmonics in Sec. 2, reversible structural transformation and carrier-density manipulation are the common strategies for smart windows because of highly reversible intensity control of transparency in the wavelength of visible and NIR ranges. Here, we summarize the main properties of smart windows enabled by electrochemical deposition/stripping and capacitive charging.[34–36,79,102]

The key parameters of smart windows are summarized in Table 1, including the employed materials, approaches,

Table 1 Summary of smart windows of various approaches.

Material	WO$_3$[102]	Cu-Ag[34]	Cu-Bi, NiO[35]	ITO[82]	AZO[82]
Approach	Ion insertion	Electrochemical deposition	Electrochemical deposition and ion insertion	Capacitive charging	Capacitive charging
Mechanism	Polaronic absorption	Structural transformation	Structural transformation	Carrier-density change	Carrier-density change
Device area	—	25 cm^2	100 cm^2	4 cm^2	4 cm^2
Spectral range	VIS	400 to 1000 nm	VIS	NIR	NIR
ΔT	97.7% (633 nm)	75% (600 nm)	65% (600 nm)	25% (solar NIR)	40% (solar NIR)
Switch speed coloration/ bleaching	6 s/2.7 s	<3 min	60 s	3.06 s/6.8 s 0.1 M LiCO$_4$/PC	1 s/1.8 s 0.1 M LiCO$_4$/PC
Coloration efficiency (cm^2 C^{-1}) (for contrast ratio at a specific wavelength)	118.3 (for 97.7% at 633 nm)	90 (for 60% at 600 nm)	—	400 (for ~60% at 1800 nm)	450 (for ~57% at 2000 nm)
Cycling	300	5500	4000	20,000, 45% capacity decay	20,000, 11% capacity decay

mechanisms, device area, adjustable spectral range, transmittance, switch speed, coloration efficiency, and cycling stability. It is worth noting that the coloration efficiency is defined as the ratio of optical density change and electric charge inserted into materials. The high coloration efficiency is pursued because the higher coloration efficiency means lower energy consumption. Four systems of plasmonic smart windows are summarized, including Cu-Ag and Cu-Bi electrochemical deposition devices,[34,35] ITO and AZO metal oxide systems.[82] WO_3 electrochromic-based smart windows are included as the baseline to compare the development of dynamic plasmonics-based smart windows.[102] We discuss them in the following part in detail.

The commonly used traditional electrochromic material is WO_3. The dynamic switch happens between the colorless state and the colorful blue state through ion insertion. The physical mechanism for color change is that, upon ion insertion with the external voltage, the injected electrons can occupy the empty d band and be localized at metal sites, which leads to the polaronic absorption and transparency change through intraband transitions. Research studies reveal that porous WO_3 exhibits large optical contrast modulation (97.7% at 633 nm), fast switching kinetics [t (coloration time) = 6 s, t (bleaching time) = 2.7 s], good cycling stabilities (100% after 300 cycles), and high coloration efficiency (118.3 $cm^2 C^{-1}$ at 633 nm).[102] The effects of the hybrid, doping, and crystal structures on WO_3 smart windows are reviewed in the literature.[102]

Electrodeposition enabled dynamic plasmonics for smart windows shows the advantages of the neutral color at dark states compared with the conventional blue appearance of WO_3-based smart windows. The long path of ions transported from the counter electrode to the center of the deposition substrate is the critical limiting step of the switch speed and uniformity for large size devices. To improve the switching speed, Islam et al.[35] designed a plane-parallel structure device (rather than a metal frame around the device perimeter for the traditional design) for 100 cm^2 smart windows with a fast switching speed. The Bi and Cu deposition at the working electrode forms rough surfaces at the nanometer scale, leading to plasmon absorption and light trapping, thus resulting in an opaque black state. The counter electrode is an anodically coloring material ($LiNiO_x$, 200-nm thick) with 15% contrast ratio of transparency at 600 nm between lithiation and delithiation states. In 60 s, the 100-cm^2 smart windows uniformly switch from a clear state with 75% transmission to a color neutral black state possessing 10% transmission at 600 nm. The same transmittances at the center and edge of the device highlight that the window switches to its dark state uniformly, indicating the reliability of plane-parallel devices. The 100-cm^2 smart windows can cycle for at least 4000 times without degradation. The coloration efficiency of electrochemical deposition enabled smart window is 90 $cm^2 C^{-1}$ at 600 nm for the Cu-Ag system, which is lower than for porous WO_3. In the future, more attention should be paid on improving the coloration efficiency by choosing optimal deposition materials and electrolyte systems.

The second category of material for smart windows is the metal-doped transition metal oxide, including ITO and AZO. As we discussed earlier, capacitive charging can change the carrier density of plasmonic materials and thus change the plasmonic resonance and spectra transmittance. ITO shows the fast switching speed [t (coloration time) = 3.06 s, t (bleaching time) = 6.8 s], high coloration efficiency (400 $cm^2 C^{-1}$ at 1800 nm), and good cycling stability (45% capacity decay after

20,000 cycles).[82] AZO shows better overall performances, with faster switching speed [t (coloration time) = 1 s, t (bleaching time) = 1.8 s], better cycling stability (11% capacity decay after 20,000 cycles), and higher coloration efficiency (450 $cm^2 C^{-1}$ at 2000 nm).[82] The limitation of doped transition metal oxide-based smart windows is the limited optical contrast in the wavelength range of the NIR solar spectrum (less than 40%). For a discussion of principles, including the doping, size, and material selection, for nanocrystal-based plasmonic smart windows please see Ref. 79.

Even though rapid progresses have been achieved in the field of dynamic plasmonics-based smart windows, there are challenges that need to be addressed in the future. For instance, we need to develop advanced smart windows with higher modulation intensity, less angular and polarization dependence, lower material cost, and higher durability. In addition, it is important to flexibly manipulate full blackbody irradiance spectrum ranges with the target of maximum energy saving for smart windows of the future.

3.2 Structural Color Displays

The second promising application field for dynamic plasmonics is structural color displays. Display technologies have widely permeated our daily life for flexible visual information, which are either based on intensity modulation or color switching with three primary colors generating subpixels, red-green-blue (RGB) or cyan-magenta-yellow (CMY). The traditional electronic display technologies are liquid crystal displays (LCDs), organic light-emitting diodes, and electrophoretic displays.[103–105] Dynamic plasmonics with flexible tuning optical responses in the visible wavelength range for structure color meets the requirements for displays, which may have potential applications for information displays. Because of their unique capability of steering the intensity and resonant wavelength with subwavelength-sized structures, plasmonic color displays may provide advanced technologies toward ultrahigh pixel resolution and never color fading compared with traditional displays.[29,106–108]

Among the three main above-discussed approaches for dynamic plasmonics, structural transformation and electrochemically active surrounding-media manipulation mechanisms show the best ability to control the intensity and resonant wavelength of optical spectra in the visible wavelength range. Thus, reversible dynamic plasmonics based on structural transformation and electrochemically active surrounding-media manipulation both can demonstrate superior overall performance of structural color displays. The key parameters related to displays are summarized in Table 2, including the materials, approaches, mechanisms, spectral range/tunability, reflectivity, speed, resolution, angle independence, cycling stability, and energy consumption. Four plasmonic structures, including Au/Ag core–shell nanodomes,[32] Au-WO_3-Au nanohole cavities,[37] PANI-coated Au nanoparticles on the Au mirror,[57] and LC on Al nanowell structures,[26] are discussed in detail in the following part.

Electrochemical deposition can reach the widest range of modulation spectra (220 nm) in Au/Ag core–shell nanodome structures. Electrochemical deposition can change the shape of the plasmonic structure and thus change the resonance wavelength. Ag deposition on Au nanoparticles can form Au/Ag core–shell nanodomes.[32] Controlling the deposition time and thickness of the Ag shell, the reflectance peak is shifted from 430 to 650 nm with 60% reflectance intensity. The refresh speed

Table 2 Summary of structural color displays of various approaches.

Structure	Au/Ag core shell nanodome[32]	Au-WO$_3$-Au nanohole cavities[37]	PANI-coated Au nanoparticle on Au mirror[57]	LC on Al nanowell[26]
Approach	Electrochemical deposition	Li ion insertion into WO$_3$	Redox reaction of polymer	LCs orientation change
Mechanism	Structural transformation	Surrounding refractive index change	Surrounding refractive index change	Surrounding refractive index change
Spectral range/ tunability	220-nm shift	64-nm shift	>100-nm shift	95-nm shift
Reflectivity	60%	35%	>50%	50% to 80%
Speed	<1 s	4 s	30 ms	Millisecond-scale
Resolution	—	5×10^4 pixels/inch	>10^9 pixels/inch	High
Angle independence	—	—	Yes	20 deg
Stability, retention	—	100 cycles, 88%	>3 months	—
Energy consumption	—	5.6 mW cm^{-2}	0.3 mW cm^{-2}	—

is <1 s for a 10×10 display screen showing "S"-"Y"-"S" letters with all 100 cells operated simultaneously. The drawback for the electrochemical deposition enabled display technology is the limited cycling stability, which calls for strict requirements for the reversible transformation of structure morphology during cycling. New technologies need to be developed to stabilize the deposited metal structure during long cycling for stable displays.

Steering the refractive index of surrounding materials of plasmonic structures can also change the resonance wavelength, thus tuning the display colors. The refractive index of inorganic electrochromic materials and polymers can be adjusted by electrochemical reactions, which all show applications for displays.

Applying inorganic electrochromic materials WO$_3$ as the insulator layer in the Au-WO$_3$-Au nanohole cavities structure can realize displays.[37] With Li ion insertion into WO$_3$ by an external voltage, a 64-nm shift of resonance wavelength and 35% reflectance intensity can be achieved in 4 s. The display resolution can reach more than 5×10^4 pixels per inch. The display devices can last 100 cycles with 88% capacity retention under the low energy consumption of 5.6 mW cm^{-2}.

Very recently, the lowest energy consumption of the dynamic plasmonic-based display is achieved in the structure of PANI-coated Au nanoparticles on an Au mirror [Fig. 5(a)]. As discussed in Sec. 2.3, PANI-coated Au nanoparticles on an Au mirror can enable >100 nm wavelength shifts due to redox reactions of polymers.[57] Dark field images of Au nanoparticles with 20-, 40-, and 60-nm diameters during PANI redox reactions show distinct color changes [Figs. 5(b) and 5(c)]. Employing this PANI-coated Au nanoparticle on an Au mirror for displays, >50% optical contrast, 30-ms switching time, and low energy consumption (0.3 mW cm^{-2}, 9 fJ per pixel) can be achieved. Due to the small particle size, the resolution of this PANI-coated Au nanoparticles enabled display can reach <100 nm, which means high pixel densities of >10^9 pixels per inch. In addition, this PANI-coated Au nanoparticle on the

Au mirror display is not sensitive to light illumination and view angles. The display devices can last for more than 3 months without degradation [Fig. 5(d)]. The switching times of various nanomaterials for plasmonic display are compared in Figs. 5(e) and 5(f) versus wavelength and pixel areas, proving that it is highly competitive with current technologies (a few to tens of ms).[109]

As the goal for future study, it is important for dynamic plasmonic displays tuned by surrounding refractive index change to increase the shift range of resonance wavelength for each pixel. Now, the spectral shift is limited to 100 nm for one pixel among all three structures, which means that full color cannot be realized using merely one pixel. Researchers need to develop new designs, for example, explore optimal materials or new dynamic manipulation mechanisms, to increase the spectral shift range of each pixel, providing full spectrum displays to replace the three color-generating RGB or CMY subpixels of current display panels.

Lastly, we also summarize the progresses of LC-enabled displays even though they belong to the pure electrical control field. The reason is that there are similarities of LC-enabled displays with electrochemically controlled plasmonic displays, and the rapid progress of LC-enabled displays can promote the development of electrochemically controlled plasmonic displays. The orientation of LCs can be adjusted with the applied voltage to control the dielectric constant of surrounding materials of the metallic nanostructures and hence determine the plasmon resonance wavelength to realize dynamic plasmonics. LCs on Al nanowells show a 95-nm spectrum shift with 50% to 80% absolute intensity of reflection peaks.[26] The switching time was in the millisecond scale. The plasmonic structure shows angle independence up to 20 deg.[26] Furthermore, full color can be realized in a single plasmonic pixel with polarization-dependent plasmonic resonances combined with LC and plasmonic rough Al surfaces.[87] Franklin et al.[87] connected the LC-assisted plasmonic displays with conventional transmissive twisted-nematic
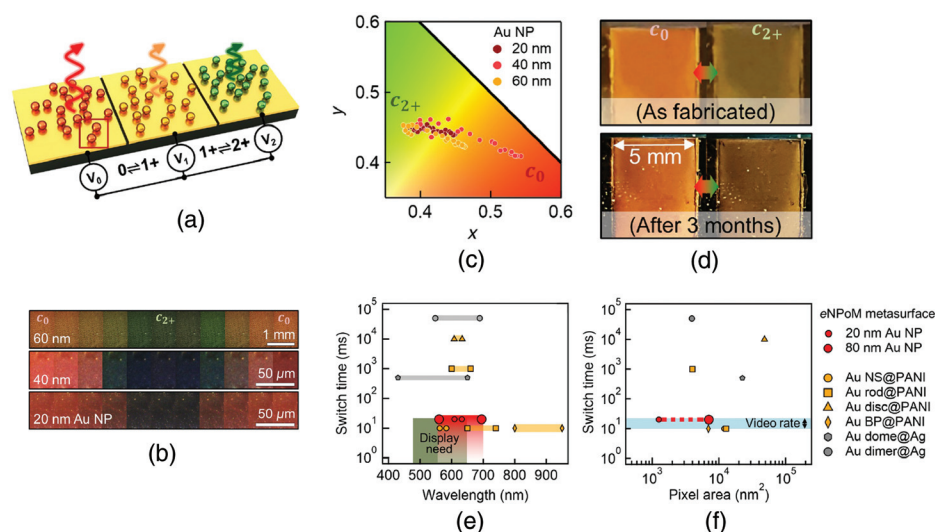
Fig. 5 Applications of dynamic plasmonics: structural color displays. (a) Schematic of PANI-coated Au nanoparticles-based displays integrated with an electrochemical cell for scalable color generation. (b) Dark field images of Au nanoparticles with 20-, 40-, and 60-nm diameters during PANI redox reactions. (c) Color gamut (CIE 1931 chromaticity) of PANI-coated Au nanoparticles with 20-, 40-, and 60-nm diameters during PANI redox. (d) Device photo of PANI-coated Au nanoparticles before and after 3 months. Switching times of various plasmonic nanomaterials versus (e) the wavelength and (f) pixel areas. (a)–(f) Reproduced with permission from Ref. 57, Copyright 2019, American Association for the Advancement of Science.

LCD paneling to realize arbitrary images and video, proving that this plasmonic display technology is compatible with present commercial LCD technologies through integration with a thin-film-transistor array.

3.3 Chemical Sensors

The third intriguing application field of dynamic plasmonics is chemical sensors. As discussed in Sec. 2, structure parameters and properties of the surrounding materials can strongly affect the plasmonic optical spectra. Thus, dynamic plasmonics based on the above-mentioned three approaches all can serve as a time-resolved optical indicator in the field of spectroelectrochemistry for chemical sensors. Here, we summarize the progresses on dynamic plasmonics enabled by carrier density and electrochemically reactive surrounding-media manipulations for sensing electrochemical reactions (including electrocatalysis reactions) and structural transformation-based dynamic plasmonics as lithium metal batteries sensors, respectively.

First, based on the established relationship between the charge density or the refractive index and the resonance wavelength, quantitative analysis of the spectral shift can be used to calculate the charge density on plasmonic particles or the refractive index of surrounding materials. In addition, dynamic plasmonics can be regarded as a ruler to measure the electrochemical behavior and the related electrochemical reaction product on the single particle level, beneficial for the understanding of catalysis mechanisms [Fig. 6(a)]. For the electrocatalysis oxidation reaction of H_2O_2 on a single gold nanoparticle surface [Fig. 6(b)], the resonant peak shifts of scattering spectra can reveal the surface information of a single gold nanoparticle during the electrocatalytic process [Figs. 6(c) and 6(d)].[110] For more details about plasmonic sensing, refer to Ref. 111.

In addition, the correlation between the structural transformation (including particle assembly/disassembly and electrochemical metal deposition/stripping) and spectrum modulation can be the basic principle for chemical sensors. Dynamic plasmonics enabled by nanoparticle assembly/disassembly can generate the application of tunable surface-enhanced Raman spectroscopy for trace chemical detection.[112–114] More importantly, electrochemical metal deposition/stripping-enabled dynamic plasmonics can serve as the operando monitoring platform for observing the change of metal morphologies during deposition and stripping processes, which is particularly important for the metal anode of metal batteries.

At the intersection of alkali-based dynamic plasmonics and alkali metal batteries, achievements and applications can be demonstrated in both fields. Lithium-based dynamic plasmonics can be used as battery sensors, as demonstrated by Jin et al.[58] [Figs. 6(e)-6(j)]. For the application of the battery sensor, as we discussed before, ordered lithium particles and undesired lithium dendrites show totally different reflectance spectra, which is the theoretical basis for operando plasmonic monitoring. On the fundamental study level, operando plasmonic monitoring can study the lithium deposition behavior without the destruction of battery devices. We need to mention that there are many challenges for lithium metal characterizations because lithium is sensitive to electron beam irradiations and reactive in the atmospheric environment. The *in situ* dynamic platform can identify lithium deposition and stripping morphologies at different current densities in a full electrochemical cycle. Two values of electric currents ($I = 0.03$ and 1 mA) were chosen to cause lithium particle growth and lithium dendrite formation. For the case $I = 0.03$ mA, the operando reflection spectra show a clear dip at ~800 nm, indicating lithium particle growth [Fig. 6(e)]. The reflectance is reversible for the lithium particle stripping
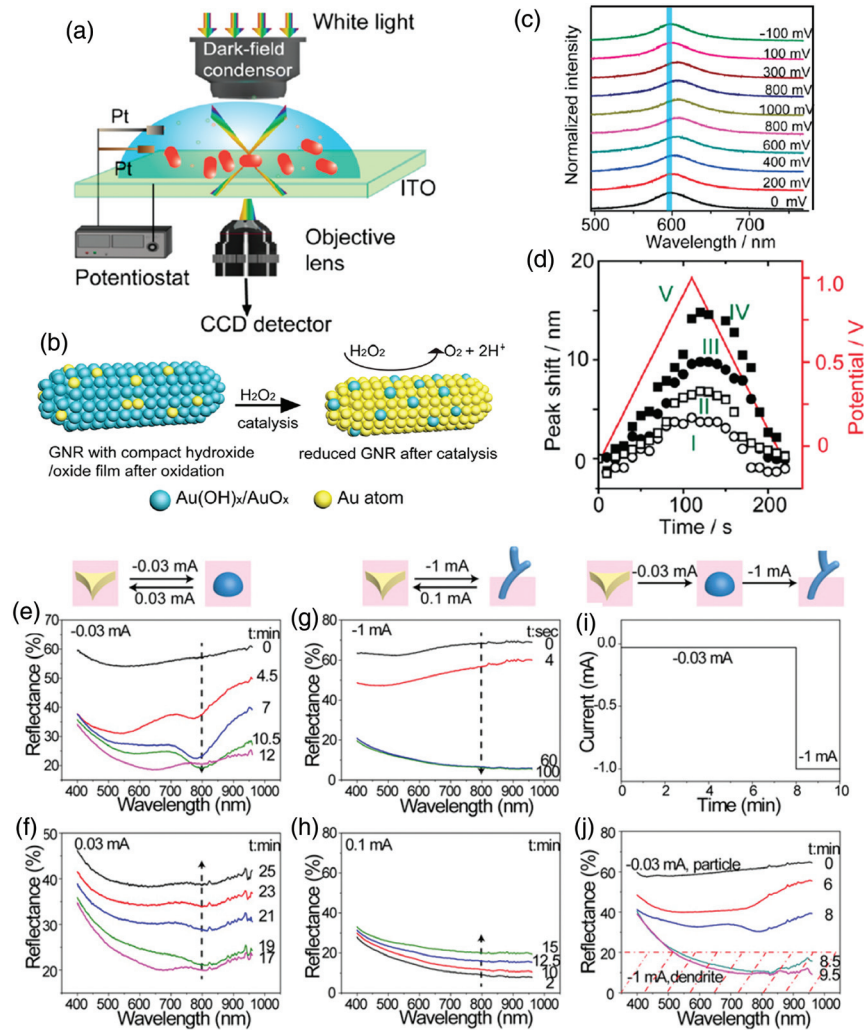
Fig. 6 Applications of dynamic plasmonics: chemical sensors. (a)–(d) Electrocatalysis reaction sensors: (a) schematic of dark-field microscopy integrated with an electrochemical workstation for chemical reaction sensors; (b) schematic of the electrocatalytic oxidation reaction mechanism of H_2O_2 on a single gold nanoparticle surface; (c) scattering spectra of a single gold nanoparticle (~40 nm × 65 nm) during the cyclic scanning; (d) scattering peak shift of 40 nm × 65 nm (I, III) and 40 nm × 84 nm (II, IV) single gold nanoparticle with (I, II) and without (III, IV) 1 mM H_2O_2 in 0.10 M KNO_3 solution under the applied potential from –0.10 to 1.00 V. (e)–(j) Battery sensors: (e)–(h) in operando reflectance during lithium metal (e), (g) deposition and (f), (h) stripping at two applied current densities: (e), (f) 0.03 mA and (g), (h) 1 mA. *In situ* lithium dendrite detection with (i) applied current and (j) *in situ* reflectance. (a)–(d) Reproduced with permission from Ref. 110, Copyright 2014, American Chemical Society. (e)–(j) Reproduced with permission from Ref. 58, Copyright 2018, National Academy of Sciences.

process [Fig. 6(f)]. For the case $I = 1$ mA, the operando reflection spectra show a rapid decrease of broadband reflectance, indicating lithium dendrite formation [Fig. 6(g)]. The reflectance is irreversible during the lithium stripping process due to the dead lithium left [Fig. 6(h)]. The accuracy of this *in-situ* reflectance-based detection for lithium morphologies is proved by *ex-situ* SEM images. Lithium deposition behavior in different electrolytes is also evaluated, which can be used as a platform for electrolyte screening. In addition, the dynamic plasmonic monitoring platform can detect *in situ* lithium dendrite formation with the sudden reflectance drop [Figs. 6(i) and 6(j)]. This method can improve the battery safety and pave the way toward

real applications of lithium metal batteries. In turn, lithium metal batteries can decrease the energy consumption of the electrochemical manipulation process for lithium metal-based dynamic plasmonics. Since the lithium metal battery is regarded as the promising ultimate energy storage technology, the external energy applied to the lithium metal deposition (charge) process can be recovered and stored, which later can be released and drive the lithium stripping (discharge) process inside the full cycles of lithium metal batteries. This is a huge benefit compared with noble metal deposition/stripping (continues external energy consumption). This lithium metal battery-based dynamic plasmonic modulation represents exciting progresses toward

low energy consumption and even self-powered dynamic plasmonic devices. However, more experimental research needs to be achieved in the future to demonstrate the concept and quantify the energy consumption.

4 Summary and Outlook

At the intersection of photonics and electrochemistry, dynamic plasmonics, achieved successfully by a variety of structures and devices, is attracting much interest in the fields of physics, chemistry, and materials science. Here, we have reviewed the rapid research progress of dynamic plasmonics enabled by electrochemical systems. We summarized three primary approaches to achieve dynamic plasmonics, including structural transformation, carrier-density modulation, and electrochemically active surrounding-media manipulation. The nanostructural design, physical mechanism, and corresponding optical property were discussed in detail. We also summarized three representative applications of dynamic plasmonics: smart windows, structural color displays, and chemical sensors.

It is of great importance to develop more stable electrochemical systems, exploring the underlying electrochemical mechanisms to meet the growing requirements of applications. In addition, electrochemical dynamic platforms with multiple functionalities or plasmonic tunabilities will be highly desired.

Optimizing materials and microstructures. Aiming at powerful dynamic plasmonics, more efforts should be devoted to stable and efficient manipulation approaches. Optimization of the conventional manipulation approaches is still urgent, such as precise defect or band structure engineering of materials, rational designing of functional plasmonic microstructures with broadband spectral tunability, or developing powerful surrounding materials with appealing electric and chemical properties. Structural transformation of the surrounding material can be a future direction to enable dynamic plasmonics, which can change the interaction or coupling between isolated plasmon resonances and may provide new insights into soft dynamic plasmonics.

Extending the manipulable degrees of freedom. In terms of the manipulation degrees of freedom, the current electrochemical dynamic plasmonics, which merely involves the modulation of intensity and wavelength, is rather limited. Dynamic plasmonics with multiple degrees of freedom for spectral manipulation will be urgently provided. Such endeavors will greatly promote applications in the fields of chemical sensing, structure color displays, and other information areas.

Broadening the optical window. In order to fully meet the requirements of the next-generation active devices across a broader wavelength range, developing new electrochemically tunable materials and microstructures, as well as their functional integration, is rather critical. For smart windows, it is important to separately manipulate the spectrum ranges of the visible and NIR wavelengths to manage indoor lighting and heat, respectively. For displays, the chemical shift is lower than 100 nm for each pixel, based on most approaches proposed up to now. A broadened wavelength shift range with new structure designs and new manipulation mechanisms to cover the wavelength of three color-generating RGB or CMY subpixels is still urgently needed.

Accelerating commercial applications. More effort should be devoted to multiple figures of merit beyond performance. Mass production of these dynamic plasmonic structures with low cost is still a challenge. Nano- and laser printing may be possible ways to achieve mass production. Decreasing energy consumption for dynamic plasmonic modulation during electrochemical processes is of great importance. Combining dynamic plasmonics with energy conversion and storage systems (for example, lithium batteries and solar cells) for multifunctional dynamic plasmonics is the future trend to reach self-powered devices. In addition, better device design from the perspective of real application scenarios is needed. One should choose optimal counter electrodes and design the position of working electrodes and counter electrodes in the devices to fully utilize the large surface area of plasmonic working electrodes and enable fast ion transport for the fast switch speed.

In summary, it is crucial to devote more effort into more effective and efficient dynamic tuning approaches in future study. With the development of the nanomaterials and nanotechnologies, it is expected that the disciplinary interplay between nanophotonics and electrochemistry can advance the field of dynamic plasmonics and find their way towards more point-of-use applications.

References

1. S. A. Maier, *Plasmonics: Fundamentals and Applications*, Springer, New York (2007).
2. J. A. Schuller et al., "Plasmonics for extreme light concentration and manipulation," *Nat. Mater.* **9**(3), 193–204 (2010).
3. E. Ozbay, "Plasmonics: merging photonics and electronics at nanoscale dimensions," *Science* **311**(5758), 189–193 (2006).
4. D. K. Gramotnev and S. I. Bozhevolnyi, "Plasmonics beyond the diffraction limit," *Nat. Photonics* **4**(2), 83–91 (2010).
5. R. M. Ma and R. F. Oulton, "Applications of nanolasers," *Nat. Nanotechnol.* **14**(1), 12–22 (2019).
6. S. Lal, S. Link, and N. J. Halas, "Nano-optics from sensing to waveguiding," *Nat. Photonics* **1**(11), 641–648 (2007).
7. H. A. Atwater and A. Polman, "Plasmonics for improved photovoltaic devices," *Nat. Mater.* **9**(3), 205–213 (2010).
8. Y. Fang and M. Sun, "Nanoplasmonic waveguides: towards applications in integrated nanophotonic circuits," *Light: Sci. Appl.* **4**(6), e294 (2015).
9. J. Valentine et al., "Three-dimensional optical metamaterial with a negative refractive index," *Nature* **455**(7211), 376–379 (2008).
10. Z. Liu et al., "Far-field optical hyperlens magnifying sub-diffraction-limited objects," *Science* **315**(5819), 1686 (2007).
11. J. Liang et al., "Plasmon-enhanced solar vapor generation," *Nanophotonics* **8**(5), 771–786 (2019).
12. C. Chen et al., "Dual functional asymmetric plasmonic structures for solar water purification and pollution detection," *Nano Energy* **51**, 451–456 (2018).
13. L. Zhou et al., "Self-assembly of highly efficient, broadband plasmonic absorbers for solar steam generation," *Sci. Adv.* **2**(4), e1501227 (2016).
14. L. Zhou et al., "3D self-assembly of aluminium nanoparticles for plasmon-enhanced solar desalination," *Nat. Photonics* **10**(4), 393–398 (2016).

15. O. Neumann et al., "Compact solar autoclave based on steam generation using broadband light-harvesting nanoparticles," *Proc. Natl. Acad. Sci. U. S. A.* **110**(29), 11677–11681 (2013).

16. M. L. Brongersma, N. J. Halas, and P. Nordlander, "Plasmon-induced hot carrier science and technology," *Nat. Nanotechnol.* **10**(1), 25–34 (2015).

17. R. Stanley, "Plasmonics in the mid-infrared," *Nat. Photonics* **6**(7), 409–411 (2012).

18. R. Chikkaraddy et al., "Single-molecule strong coupling at room temperature in plasmonic nanocavities," *Nature* **535**(7610), 127–130 (2016).

19. E. C. Garnett et al., "Self-limited plasmonic welding of silver nanowire junctions," *Nat. Mater.* **11**(3), 241–249 (2012).

20. C. Caucheteur et al., "Ultrasensitive plasmonic sensing in air using optical fibre spectral combs," *Nat. Commun.* **7**(1), 13371 (2016).

21. N. Jiang, X. Zhuo, and J. Wang, "Active plasmonics: principles, structures, and applications," *Chem. Rev.* **118**(6), 3054–3099 (2017).

22. X. Duan and N. Liu, "Magnesium for dynamic nanoplasmonics," *Acc. Chem. Res.* **52**(7), 1979–1989 (2019).

23. L. Ju et al., "Graphene plasmonics for tunable terahertz metamaterials," *Nat. Nanotechnol.* **6**(10), 630–634 (2011).

24. Z. Fei et al., "Gate-tuning of graphene plasmons revealed by infrared nano-imaging," *Nature* **487**(7405), 82–85 (2012).

25. A. N. Grigorenko, M. Polini, and K. S. Novoselov, "Graphene plasmonics," *Nat. Photonics* **6**(11), 749–758 (2012).

26. D. Franklin et al., "Polarization-independent actively tunable colour generation on imprinted plasmonic surfaces," *Nat. Commun.* **6**(1), 7337 (2015).

27. L. Liu et al., "Dynamic color-switching of plasmonic nanoparticle films," *Angew. Chem.* **131**(45), 16453–16459 (2019).

28. N. Liu and T. Liedl, "DNA-assembled advanced plasmonic architectures," *Chem. Rev.* **118**(6), 3032–3053 (2018).

29. X. Duan, S. Kamin, and N. Liu, "Dynamic plasmonic colour display," *Nat. Commun.* **8**(1), 14606 (2017).

30. F. Sterl et al., "Magnesium as novel material for active plasmonics in the visible wavelength range," *Nano Lett.* **15**(12), 7949–7955 (2015).

31. A. Tsuboi, K. Nakamura, and N. Kobayashi, "A localized surface plasmon resonance-based multicolor electrochromic device with electrochemically size-controlled silver nanoparticles," *Adv. Mater.* **25**(23), 3197–3201 (2013).

32. G. Wang et al., "Mechanical chameleon through dynamic real-time plasmonic tuning," *ACS Nano* **10**(2), 1788–1794 (2016).

33. K. Xiong et al., "Plasmonic metasurfaces with conjugated polymers for flexible electronic paper in color," *Adv. Mater.* **28**(45), 9956–9960 (2016).

34. C. J. Barile et al., "Dynamic windows with neutral color, high contrast, and excellent durability using reversible metal electrodeposition," *Joule* **1**(1), 133–145 (2017).

35. S. M. Islam et al., "Hybrid dynamic windows using reversible metal electrodeposition and ion insertion," *Nat. Energy* **4**(3), 223–229 (2019).

36. P. Pattathil, R. Giannuzzi, and M. Manca, "Self-powered NIR-selective dynamic windows based on broad tuning of the localized surface plasmon resonance in mesoporous ITO electrodes," *Nano Energy* **30**, 242–251 (2016).

37. E. Hopmann and A. Y. Elezzabi, "Plasmochromic nanocavity dynamic light color switching," *Nano Lett.* **20**(3), 1876–1882 (2020).

38. Z. Zhang et al., "Thermo-optic coefficients of polymers for optical waveguide applications," *Polymer* **47**(14), 4893–4896 (2006).

39. G. M. Koenig et al., "Coupling of the plasmon resonances of chemically functionalized gold nanoparticles to local order in thermotropic liquid crystals," *Chem. Mater.* **19**(5), 1053–1061 (2007).

40. M. Liu et al., "Terahertz-field-induced insulator-to-metal transition in vanadium dioxide metamaterial," *Nature* **487**(7407), 345–348 (2012).

41. M. Toma et al., "Active control of SPR by thermoresponsive hydrogels for biosensor applications," *J. Phys. Chem. C* **117**(22), 11705–11712 (2013).

42. M. Nguyen et al., "Engineering thermoswitchable lithographic hybrid gold nanorods as plasmonic devices for sensing and active plasmonics applications," *ACS Photonics* **2**(8), 1199–1208 (2015).

43. Y. Ma et al., "Auxetic thermoresponsive nanoplasmonic optical switch," *ACS Appl. Mater. Interfaces* **11**(25), 22754–22760 (2019).

44. M. L. Tseng et al., "Two-dimensional active tuning of an aluminum plasmonic array for full-spectrum response," *Nano Lett.* **17**(10), 6034–6039 (2017).

45. P. Gutruf et al., "Mechanically tunable dielectric resonator metasurfaces at visible frequencies," *ACS Nano* **10**(1), 133–141 (2016).

46. M. Miyata et al., "Electromechanically tunable plasmonic nanowires operating in visible wavelengths," *ACS Photonics* **3**(12), 2268–2274 (2016).

47. N. I. Zheludev and E. Plum, "Reconfigurable nanomechanical photonic metamaterials," *Nat. Nanotechnol.* **11**(1), 16–22 (2016).

48. T. Okamoto, T. Kamiyama, and I. Yamaguchi, "All-optical spatial light modulator with surface plasmon resonance," *Opt. Lett.* **18**(18), 1570–1572 (1993).

49. J. Dintinger et al., "Terahertz all-optical molecule-plasmon modulation," *Adv. Mater.* **18**(13), 1645–1648 (2006).

50. M. I. Stockman, "Spasers explained," *Nat. Photonics* **2**(6), 327–329 (2008).

51. J. Zhang, K. F. MacDonald, and N. I. Zheludev, "Controlling light-with-light without nonlinearity," *Light: Sci. Appl.* **1**(7), e18 (2012).

52. M. Wang et al., "Magnet ic tuning of plasmonic excitation of gold nanorods," *J. Am. Chem. Soc.* **135**(41), 15302–15305 (2013).

53. M. Zhang et al., "High-strength magnetically switchable plasmonic nanorods assembled from a binary nanocrystal mixture," *Nat. Nanotechnol.* **12**(3), 228–232 (2017).

54. H. Li et al., "Single-stimulus-induced modulation of multiple optical properties," *Adv. Mater.* **31**(23), 1900388 (2019).

55. I. Jung et al., "Fourier transform surface plasmon resonance of nanodisks embedded in magnetic nanorods," *Nano Lett.* **18**(3), 1984–1992 (2018).

56. C. J. Dahlman et al., "Spectroelectrochemical signatures of capacitive charging and ion insertion in doped anatase titania nanocrystals," *J. Am. Chem. Soc.* **137**(28), 9160–9166 (2015).

57. J. Peng et al., "Scalable electrochromic nanopixels using plasmonics," *Sci. Adv.* **5**(5), eaaw2205 (2019).

58. Y. Jin et al., "In operando plasmonic monitoring of electrochemical evolution of lithium metal," *Proc. Natl. Acad. Sci. U. S. A.* **115**(44), 11168–11173 (2018).

59. Y. Jin et al., "Electrical dynamic switching of magnetic plasmon resonance based on selective lithium deposition," *Adv. Mater.* **32**(42), 2000058 (2020).

60. A. Boltasseva and H. A. Atwater, "Low-loss plasmonic metamaterials," *Science* **331**(6015), 290–291 (2011).

61. M. G. Blaber et al., "Plasmon absorption in nanospheres: a comparison of sodium, potassium, aluminium, silver and gold," *Phys. B* **394**(2), 184–187 (2007).

62. Y. Wang et al., "Stable, high-performance sodium-based plasmonic devices in the near infrared," *Nature* **581**(7809), 401–405 (2020).

63. J. Liu et al., "Pathways for practical high-energy long-cycling lithium metal batteries," *Nat. Energy* **4**(3), 180–186 (2019).

64. D. Lin, Y. Liu, and Y. Cui, "Reviving the lithium metal anode for high-energy batteries," *Nat. Nanotechnol.* **12**(3), 194–206 (2017).

65. C. Niu et al., "Self-smoothing anode for achieving high-energy lithium metal batteries under realistic conditions," *Nat. Nanotechnol.* **14**(4), 594–601 (2019).

66. W. Xu et al., "Lithium metal anodes for rechargeable batteries," *Energy Environ. Sci.* **7**(2), 513–537 (2014).

67. Y. Montelongo et al., "Electrotunable nanoplasmonic liquid mirror," *Nat. Mater.* **16**(11), 1127–1135 (2017).

68. D. Sikdar et al., "Electrochemical plasmonic metamaterials: towards fast electro-tuneable reflecting nanoshutters," *Faraday Discuss.* **199**, 585–602 (2017).

69. D. Sikdar and A. A. Kornyshev, "An electro-tunable Fabry–Perot interferometer based on dual mirror-on-mirror nanoplasmonic metamaterials," *Nanophotonics* **8**(12), 2279–2290 (2019).

70. D. Sikdar, H. Weir, and A. A. Kornyshev, "Optical response of electro-tuneable 3D superstructures of plasmonic nanoparticles self-assembling on transparent columnar electrodes," *Opt. Express* **27**(19), 26483–26498 (2019).

71. Y. Ma et al., "A tunable nanoplasmonic mirror at an electrochemical interface," *ACS Photonics* **5**(11), 4604–4616 (2018).

72. J. J. Mock et al., "Probing dynamically tunable localized surface plasmon resonances of film-coupled nanoparticles by evanescent wave excitation," *Nano Lett.* **12**(4), 1757–1764 (2012).

73. D. Sikdar and A. A. Kornyshev, "Theory of tailorable optical response of two-dimensional arrays of plasmonic nanoparticles at dielectric interfaces," *Sci. Rep.* **6**(1), 33712 (2016).

74. D. Sikdar et al., "Unravelling the optical responses of nanoplasmonic mirror-on-mirror metamaterials," *Phys. Chem. Chem. Phys.* **18**(30), 20486–20498 (2016).

75. A. A. Kornyshev, "Electrochemical metamaterials," *J. Solid State Electrochem.* **24**(9), 2101–2111 (2020).

76. J. B. Edel et al., "Fundamentals and applications of self-assembled plasmonic nanoparticles at interfaces," *Chem. Soc. Rev.* **45**(6), 1581–1596 (2016).

77. J. B. Edel, A. A. Kornyshev, and M. Urbakh, "Self-assembly of nanoparticle arrays for use as mirrors, sensors, and antennas," *ACS Nano* **7**(11), 9526–9532 (2013).

78. S. G. Booth et al., "Electrochemical modulation of SERS at the liquid/liquid interface," *Chem. Commun.* **50**(34), 4482–4484 (2014).

79. E. L. Runnerstrom et al., "Nanostructured electrochromic smart windows: traditional materials and NIR-selective plasmonic nanocrystals," *Chem. Commun.* **50**(73), 10555–10572 (2014).

80. A. Henglein, P. Mulvaney, and T. Linnert, "Chemistry of Ag aggregates in aqueous solution: non-metallic oligomeric clusters and metallic particles," *Faraday Discuss.* **92**, 31–44 (1991).

81. T. Ung et al., "Spectroelectrochemistry of colloidal silver," *Langmuir* **13**(6), 1773–1782 (1997).

82. G. Garcia et al., "Near-infrared spectrally selective plasmonic electrochromic thin films," *Adv. Opt. Mater.* **1**(3), 215–220 (2013).

83. B. S. Hoener et al., "Spectral response of plasmonic gold nanoparticles to capacitive charging: morphology effects," *J. Phys. Chem. Lett.* **8**(12), 2681–2688 (2017).

84. C. Novo et al., "Electrochemical charging of single gold nanorods," *J. Am. Chem. Soc.* **131**(41), 14664–14666 (2009).

85. A. M. Brown, M. T. Sheldon, and H. A. Atwater, "Electrochemical tuning of the dielectric function of Au nanoparticles," *ACS Photonics* **2**(4), 459–464 (2015).

86. T. Xu et al., "High-contrast and fast electrochromic switching enabled by plasmonics," *Nat. Commun.* **7**(1), 10479 (2016).

87. D. Franklin et al., "Actively addressed single pixel full-colour plasmonic display," *Nat. Commun.* **8**(1), 15209 (2017).

88. Y. Lee et al., "Electrical broad tuning of plasmonic color filter employing an asymmetric-lattice nanohole array of metasurface controlled by polarization rotator," *ACS Photonics* **4**(8), 1954–1966 (2017).

89. J. Olson et al., "High chromaticity aluminum plasmonic pixels for active liquid crystal displays," *ACS Nano* **10**(1), 1108–1117 (2016).

90. C. P. Byers et al., "From tunable core–shell nanoparticles to plasmonic drawbridges: active control of nanoparticle optical properties," *Sci. Adv.* **1**(11), e1500988 (2015).

91. R. Sardar et al., "Gold nanoparticles: past, present, and future," *Langmuir* **25**(24), 13840–13851 (2009).

92. B. S. Hoener et al., "Spectroelectrochemistry of halide anion adsorption and dissolution of single gold nanorods," *J. Phys. Chem. C* **120**(37), 20604–20612 (2016).

93. S. Oikawa et al., "Nanoscale control of plasmon-active metal nanodimer structures via electrochemical metal dissolution reaction," *Nanotechnology* **29**(4), 045702 (2018).

94. H. Minamimoto et al., "Electrochemical fine tuning of the plasmonic properties of Au lattice structures," *J. Phys. Chem. C* **122**(25), 14162–14167 (2018).

95. A. Al-Zubeidi et al., "Hot holes assist plasmonic nanoelectrode dissolution," *Nano Lett.* **19**(2), 1301–1306 (2019).

96. C. Flatebo et al., "Electrodissolution inhibition of gold nanorods with oxoanions," *J. Phys. Chem. C* **123**(22), 13983–13992 (2019).

97. S. Oikawa, H. Minamimoto, and K. Murakoshi, "Reversible electrochemical tuning of optical property of single Au nanobridged structure via electrochemical under potential deposition," *Chem. Lett.* **46**(8), 1148–1150 (2017).

98. Y. Jin and S. Dong, "Probing UPD-induced surface atomic rearrangement of polycrystalline gold nanofilms with surface plasmon resonance spectroscopy and cyclic voltammetry," *J. Phys. Chem. B* **107**(50), 13969–13975 (2003).

99. M. Schweizer, H. Hagenström, and D. M. Kolb, "Potential-induced structure transitions in self-assembled monolayers: ethanethiol on Au(100)," *Surf. Sci.* **490**(3), L627–L636 (2001).

100. O. Quevedo-Teruel et al., "Roadmap on metasurfaces," *J. Opt.* **21**(7), 073002 (2019).

101. Y. Ke et al., "Emerging thermal-responsive materials and integrated techniques targeting the energy-efficient smart window application," *Adv. Funct. Mater.* **28**(22), 1800113 (2018).

102. G. Cai et al., "Ultra-large optical modulation of electrochromic porous WO$_3$ film and the local monitoring of redox activity," *Chem. Sci.* **7**(2), 1373–1382 (2016).

103. Y. Huang et al., "Mini-LED, micro-LED and OLED displays: present status and future perspectives," *Light: Sci. Appl.* **9**(1), 105 (2020).

104. K. H. Kim et al., "Phosphorescent dye-based supramolecules for high-efficiency organic light-emitting diodes," *Nat. Commun.* **5**(1), 4769 (2014).

105. M. Christophersen and B. F. Phlips, "Recent patents on electrophoretic displays and materials," *Recent Pat. Nanotechnol.* **4**(3), 137–149 (2010).

106. L. Shao et al., "Advanced plasmonic materials for dynamic color display," *Adv. Mater.* **30**(16), 1704338 (2018).

107. Y. Chen et al., "Dynamic color displays using stepwise cavity resonators," *Nano Lett.* **17**(9), 5555–5560 (2017).

108. Y. Gao et al., "Lead halide perovskite nanostructures for dynamic color display," *ACS Nano* **12**(9), 8847–8854 (2018).

109. H. W. Chen et al., "Liquid crystal display and organic light-emitting diode display: present status and future perspectives," *Light: Sci. Appl.* **7**(3), 17168 (2018).

110. C. Jing et al., "New insights into electrocatalysis based on plasmon resonance for the real-time monitoring of catalytic events on single gold nanorods," *Anal. Chem.* **86**(11), 5513–5518 (2014).

111. B. S. Hoener et al., "Plasmonic sensing and control of single-nanoparticle electrochemistry," *Chem* **4**(7), 1560–1585 (2018).

112. L. Velleman et al., "Monitoring plasmon coupling and SERS enhancement through *in situ* nanoparticle spacing modulation," *Faraday Discuss.* **205**, 67–83 (2017).

113. M. P. Cecchini et al., "Self-assembled nanoparticle arrays for multiphase trace analyte detection," *Nat. Mater.* **12**(2), 165–171 (2013).

114. Y. Ma et al., "Electrotunable nanoplasmonics for amplified surface enhanced Raman spectroscopy," *ACS Nano* **14**(1), 328–336 (2020).

Yan Jin received her PhD from Nanjing University. Her research interest focuses on dynamic alkali plasmonics.

Lin Zhou is an associate professor at the College of Engineering and Applied Sciences, Nanjing University, China. She obtained her PhD from Nanjing University. Her current research interests include alkali metal plasmon photonics, solar energy conversion, and two-dimensional photonics.

Jie Liang received her bachelor's degree from Nanjing University in June 2018. She is currently pursuing her PhD at Nanjing University. Her research interest focuses on nanophotonics.

Jia Zhu is a professor at the College of Engineering and Applied Sciences, Nanjing University, China. He obtained his PhD from Stanford University and then worked as a postdoctoral fellow at the University of California, Berkeley, and at Lawrence Berkeley National Lab. His research interests include the areas of nanomaterials, nanophotonics, and nanoscale heat transfer.